The Early Evolution of the Tetrapod Humerus

Neil H. Shubin, *et al.*

Science **304**, 90 (2004);
DOI: 10.1126/science.1094295

Science (print ISSN 0036-8075; online ISSN 1095-9203) is published weekly, except the last week in December, by the American Association for the Advancement of Science, 1200 New York Avenue NW, Washington, DC 20005.

seafloor anoxia during the mid-Proterozoic was expanded compared to today during at least two intervals separated by ~300 million years. The $\delta^{97/95}$Mo data are consistent with globally extensive seafloor anoxia persisting after oxygenation of the atmosphere ~2.3 Ga. The identification of mid-Proterozoic Mn oxides with a $\delta^{97/95}$Mo value ~2‰ lighter than in coeval euxinic sediments would strengthen these arguments. Nevertheless, the full impact of nearly a billion years of ocean anoxia on Proterozoic ecosystems and biogeochemical cycles must be seriously considered.

References and Notes

1. A. H. Knoll, in *Origin and Early Evolution of the Metazoa*, J. H. Lipps, P. W. Signor, Eds. (Plenum, New York, 1992), p. 53.
2. A. D. Anbar, A. H. Knoll, *Science* **297**, 1137 (2002).
3. D. J. Des Marais *et al.*, *Astrobiology* **2**, 153 (2002).
4. H. D. Holland, *The Chemical Evolution of the Atmosphere and Oceans* (Princeton Univ. Press, Princeton, NJ, 1984).
5. H. D. Holland, *Geochem. News* **100**, 20 (1999).
6. J. Farquhar, H. Bao, M. H. Thiemens, *Science* **289**, 756 (2000).
7. D. E. Canfield, A. Teske, *Nature* **382**, 127 (1996).
8. D. E. Canfield, *Nature* **396**, 450 (1998).
9. D. E. Canfield, R. Raiswell, *Am. J. Sci.* **299**, 697 (1999).
10. A. A. Pavlov, M. T. Hurtgen, J. F. Kasting, M. A. Arthur, *Geology* **31**, 87 (2003).
11. A. J. Kaufman, S. Xiao, *Nature* **425**, 279 (2003).
12. Y. Shen, D. E. Canfield, A. H. Knoll, *Am. J. Sci.* **302**, 81 (2002).
13. Y. Shen, A. H. Knoll, M. R. Walter, *Nature* **423**, 632 (2003).
14. L. C. Kah, T. W. Lyons, J. T. Chesley, *Precambrian Res.* **111**, 203 (2001).
15. S. R. Emerson, S. S. Huested, *Mar. Chem.* **34**, 177 (1991).
16. B. E. Erickson, G. R. Helz, *Geochim. Cosmochim. Acta* **64**, 1149 (2000).
17. Y. Zheng, R. F. Anderson, A. van Geen, J. Kuwabara, *Geochim. Cosmochim. Acta* **64**, 4165 (2000).
18. J. L. Morford, S. Emerson, *Geochim. Cosmochim. Acta* **63**, 1735 (1999).
19. K. K. Bertine, K. K Turekian, *Geochim. Cosmochim. Acta* **37**, 1415 (1973).
20. J. McManus, T. F. Nagler, C. Siebert, C. G. Wheat, D. E. Hammond, *Geochem. Geophys. Geosyst.* **3**, 10.1029/2002GC000356 (2002).
21. Data are reported using the δ notation, relative to a Mo standard (Johnson Matthey Chemical, Specpure lot #702499I) where

$$\delta^{97/95}\mathrm{Mo} = \left(\frac{^{97}\mathrm{Mo}/^{95}\mathrm{Mo}_{\mathrm{sample}}}{^{97}\mathrm{Mo}/^{95}\mathrm{Mo}_{\mathrm{standard}}} - 1\right) \times 1000$$

22. J. Barling, G. L. Arnold, A. D. Anbar, *Earth Planet. Sci. Lett.* **193**, 447 (2001).
23. C. Siebert, T. F. Nagler, F. von Blanckenburg, J. D. Kramers, *Earth Planet. Sci. Lett.* **211**, 159 (2003).
24. Values reported in text are the mean ± 2 SD for all analyses of each sample grouping, unless otherwise noted.
25. Details of materials, methods, sample descriptions, and alternative hypotheses are available as supporting material on *Science* Online.
26. Molybdenite ores are assumed to consist of Mo extracted by hydrothermal processes from surrounding crustal rocks, and hence are a rough proxy for crustal Mo.
27. Siebert *et al.* (*23*) found no Mo isotope fractionation during mild acid leaching of Mo from granite and basalt. Therefore, it is reasonable to hypothesize that Mo released during crustal weathering is isotopically similar to Mo in granite, basalt, and molybdenite.
28. Although ferromanganese crusts and nodules themselves are not major sinks for Mo, a correlation of Mo and Mn is observed in pelagic sediments (*19*). This presumably reflects coprecipitation of Mo with Mn oxides on the seafloor. Hence, $\delta^{97/95}$Mo in crusts and nodules is probably representative of $\delta^{97/95}$Mo in Mn oxide–associated Mo.
29. J. Barling, A. D. Anbar, *Earth Planet. Sci. Lett.* **217**, 315 (2004).
30. G. R. Helz *et al.*, *Geochim. Cosmochim. Acta* **60**, 3631 (1996).
31. J. W. Murray, Z. Top, E. Ozsoy, *Deep-Sea Res.* **38**, S663 (1991).
32. I. H. Crick, C. J. Boreham, A. C. Cook, T. G Powell, *Am. Assoc. Petrol. Geol. Bull.* **72**, 1495 (1988).
33. T. H. Donnelly, M. J. Jackson, *Sediment. Geol.* **58**, 145 (1988).
34. D. E. Canfield, T. W. Lyons, R. Raiswell, *Am. J. Sci.* **296**, 818 (1996).
35. The use of basinal Mo concentrations to infer global ocean Mo concentrations is not straightforward, as evidenced by the nearly 10-fold difference in Mo concentrations between euxinic sediments in the Cariaco Basin and Black Sea. Local effects specific to the depositional setting presumably dominate. Hence, Mo concentrations in sediments cannot easily be used alone to draw inferences about global ocean redox conditions.
36. These figures are obtained using the following values: $\delta^{97/95}\mathrm{Mo}_{in} = -0.01$; $\Delta_{sw\text{-}ox} = 1.8$; $\delta^{97/95}\mathrm{Mo}_{eux} = 0.54$.
37. $\delta^{97/95}\mathrm{Mo}_{eux}$ of the mid-Proterozoic samples ranges from 0.31 to 0.67‰; correspondingly, the euxinic sink could range from 82 to 62%.
38. A. D. Anbar, in *Geochemistry of Non-Traditional Isotopes*, C. Johnson, B. Beard, F. Albarede, Eds. (Mineralogical Society of America, Washington, DC, 2004), pp. 429–454.
39. As an illustrative model, assume that $f_{ox} = k_{ox} \cdot A_{ox} \cdot [\mathrm{Mo}]_{sw}$ and $f_{eux} = k_{eux} \cdot A_{eux} \cdot [\mathrm{Mo}]_{sw}$, where $[\mathrm{Mo}]_{sw}$ is the concentration of Mo in the oceans, A_{ox} and A_{eux} are the areas of oxic and euxinic sedimentation, and k_{ox} and k_{eux} are proportionality constants that parameterize the partitioning of Mo between water and sediment (i.e., these constants parameterize diffusion coefficients, sedimentation rates, chemical partition functions, etc.). Hence, $f_{ox}/f_{eux} = k_{ox}/k_{eux} \cdot A_{ox}/A_{eux}$. If k_{ox} and k_{eux} are constant, then variations in f_{ox}/f_{eux} can be directly related to variations in A_{ox}/A_{eux}. The assumption of constant k_{ox} and k_{eux} is simplistic, but useful for schematic purposes.
40. Although $f_{ox} + f_{eux} = 1$, it is not necessarily the case that $A_{ox} + A_{eux} =$ constant. Hence a change in A_{ox} need not be complemented by a change in A_{eux} (and vice versa). This difference arises because a change in A_{ox} or A_{eux} can be compensated by a change in the areal extent of suboxic seafloor, whereas the Mo mass balance model assumes that suboxic sediments are a negligible sink for Mo.
41. H. D. Klemme, G. F. Ulmishek, *Am. Assoc. Petrol. Geol. Bull.* **75**, 1809 (1991).

42. We thank Y. Shen, J. Brocks, A. H. Knoll, and H. D. Holland for providing samples of Proterozoic black shales, and G. Ravizza for Black Sea samples. F. Ramos, G. Williams, and S. Weyer assisted with sample analysis. Supported by NSF (EAR 0106712 and 0230183) and NASA (Exobiology program and the Astrobiology Institute).

Supporting Online Material
www.sciencemag.org/cgi/content/full/1091785/DC1
Materials and Methods
SOM Text
Fig. S1
Tables S1 and S2
References and Notes

23 September 2003; accepted 24 February 2004
Published online 4 March 2004;
10.1126/science.1091785
Include this information when citing this paper.

The Early Evolution of the Tetrapod Humerus

Neil H. Shubin,[1]* Edward B. Daeschler,[2] Michael I. Coates[1]

A tetrapod humerus from the Late Devonian of Pennsylvania has a novel mix of primitive and derived characters. A comparative analysis of this fossil and other relevant humeri from the Devonian shows that the role of the limb in propping the body arose first in fish fins, not tetrapod limbs. The functional diversity of the earliest known limbs includes several different kinds of appendage design. This functional diversity was achieved with a humeral architecture that was remarkably conserved during the Devonian.

The evolution of limbed vertebrates from lobe-finned fish is one of the key transitions in the history of life. The origin of the tetrapod body plan has classically been associated with the invasion of land; accordingly, limbs were seen to have arisen to support and move the body in a terrestrial habitat (*1*, *2*). In recent years this view has changed with new descriptions of Devonian forms, such as *Acanthostega* (*3*, *4*). Although clearly a tetrapod, *Acanthostega* retains a variety of aquatic adaptations, including flipper-like appendages, internal gills, and a broad finned tail. Unfortunately, our limited ability to make comparisons between homologous features in the humeri of basal tetrapods and their closest fish relatives has hampered our understanding of the fin-limb transition. Theories about the origin of tetrapod limbs have relied mainly on comparisons of humeri of Carboniferous and Permian tetrapods with that of *Eusthenopteron* (*5*), a well-known Devonian lobe-finned fish. In recent years, these temporal and anatomical gaps have narrowed, with new descriptions of limbs of the basal tetrapods *Acanthostega* (*3*, *6*), *Ichthyostega* (*7*), and *Tulerpeton* (*8*) and emerging details of the pectoral fin in *Panderichthys* (*9*, *10*), the most crownward fish on the tetrapod stem

[1]Department of Organismal Biology and Anatomy, University of Chicago, Chicago, IL 60637, USA. [2]Academy of Natural Sciences, 1900 Benjamin Franklin Parkway, Philadelphia, PA 19103, USA.

*To whom correspondence should be addressed. E-mail: nshubin@uchicago.edu

lineage. Here we describe a tetrapod humerus that provides the basis for new interpretations of structural and functional stages in the origin of the tetrapod limb.

The new humerus, ANSP 21350, (Fig. 1) was recovered from the upper part of the Catskill Formation at the Red Hill locality in north central Pennsylvania. Palynomorph biostratigraphy indicates that the site is from the late part of the Famennian Stage (Fa2c) of the Upper Devonian (*11*). The specimen comes from channel margin deposits within a sequence of fluvial sediments. A diverse assemblage of plants, invertebrates, and vertebrates, including other early tetrapod material, has been recovered from Red Hill. ANSP 21350 is the only limb element recovered from the site. The new humerus comes from the same 1-m-wide lens that produced material of *Hynerpeton* (*12*), but the size of ANSP 21350 is about 50% larger than would be expected for *Hynerpeton*, based on two similarly sized left shoulder girdles. *Densignathus* (*13*), a larger tetrapod from the Red Hill site, is known only from lower jaw material from the same stratigraphic level about 50 m from where the new humerus was found. Consequently, we are unable to discern whether the new humerus is referable to *Hynerpeton*, *Densignathus*, or a third tetrapod taxon.

Our identification of ANSP 21350 as a tetrapod humerus is based on the presence of multiple shared derived features also seen in *Acanthostega* (Fig. 2), *Ichthyostega* (*7*), and *Tulerpeton* (*8*). These features include an L-shaped external outline in ventral or dorsal view (*4*), a distally extended ectepicondylar process (Fig. 1, ectc; Fig. 2, no. 7), a recess and incipient crest at the proximal union of ectepicondylar and entepicondylar processes (Fig. 2, no. 10), and a ventral ridge that runs nearly perpendicular to the long axis of the humeral shaft (Fig. 1 vnt; Fig. 2, no. 3). ANSP 21350, however, has several characters that are either unique or are narrowly distributed among other basal tetrapods. The posteromedial rim of the entepicondylar process is peculiarly robust and is drawn into dorsal and ventral processes that are otherwise seen most clearly in *Ichthyostega* (*7*) (Fig. 1, entc). The ectepicondylar process extends more distally than in any other known early humerus, and the ventral ridge of ANSP 21350 is extraordinarily prominent and deeply sculpted. Primitive characters are also evident in the humerus. A distinct ventral ridge dominates the humerus of tristichopterid fish such as *Eusthenopteron* (Fig. 2, no. 3), where it runs diagonally across the ventral portion of the shaft. As in ANSP 21350, this ridge is continuous with the entepicondylar process and contains a homologous set of foramina on its proximal and distal margins. The presence of this primitive arrangement is particularly striking in a tetrapod humerus that is derived in other respects.

Panderichthyids and the most basal tetrapods underwent a reorganization of the upper limb in the Late Devonian. Compared to outgroups, *Panderichthys*, ANSP 21350, and *Acanthostega* (Fig. 2, anterior views) share a humeral shaft that is greatly flattened dorsoventrally. Along with this flattening, the humeral shaft contains expanded areas for muscle insertion on the dorsal surface both proximally and distally. The humeral head, either ball-shaped or ovoid in tristichopterid, osteolepid, and rhizodontid fish (*4*, *5*), becomes anteroposteriorly elongate and dorsoventrally flattened in *Panderichthys*, *Acanthostega*, and ANSP 21350. In the shoulder, the coracoid plate is expanded in the region where flexor muscles would attach. These features indicate that important shifts had already occurred before the origin of tetrapod limbs with digits (*9*). Flattening of the humerus dorsoventrally implies that the flexor and extensor muscles have separated more com-

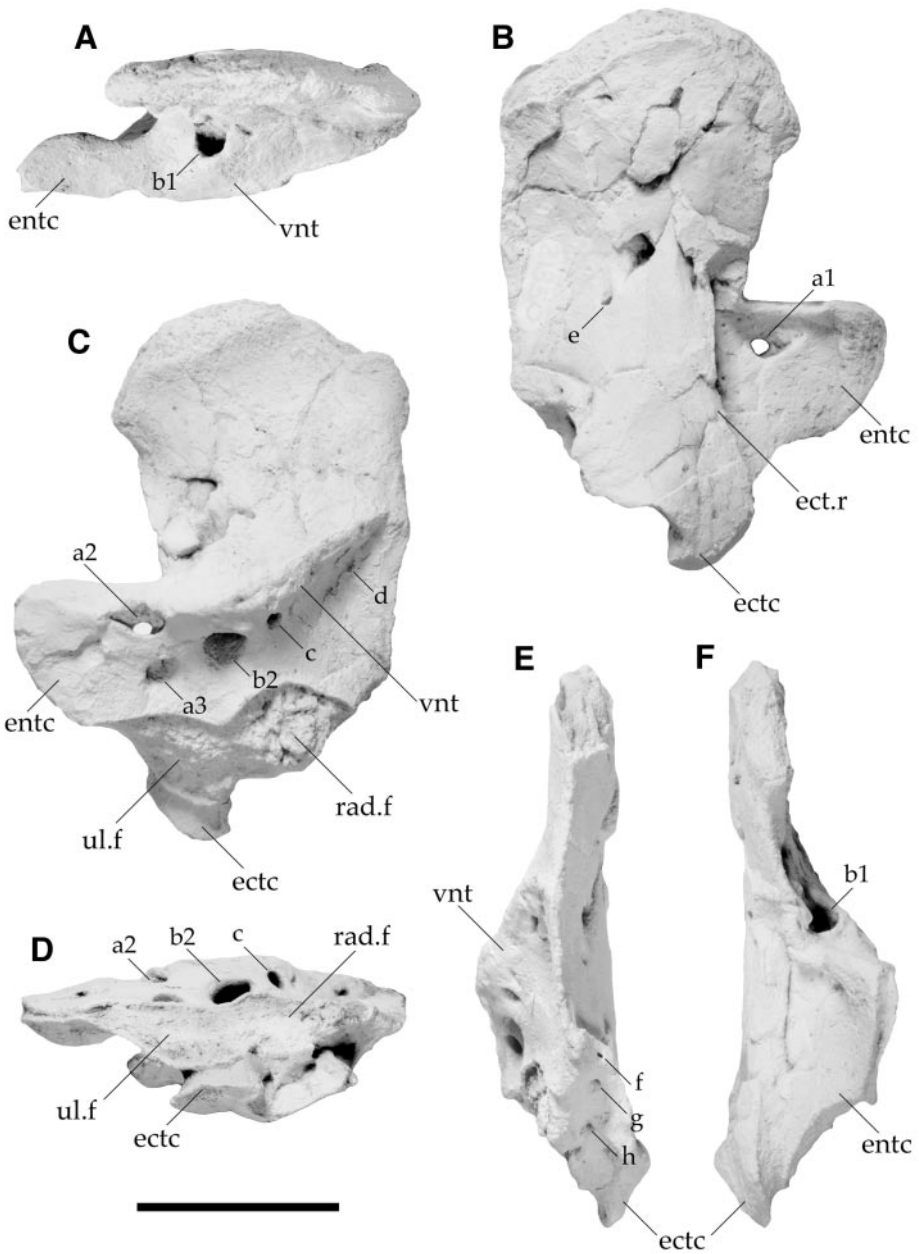

Fig. 1. ANSP 21350, the left humerus of an early tetrapod from the Late Devonian of Pennsylvania. (**A**) Proximal, (**B**) dorsal, (**C**) ventral, (**D**) distal (ventral surface is uppermost), (**E**) cranial, and (**F**) caudal views. The specimen was whitened with ammonium chloride. Abbreviations are as follows: ANSP, Academy of Natural Sciences of Philadelphia; entc, entepicondyle; vnt, ventral ridge; ect.r, ectepicondylar ridge; ectc, ectepicondyle; ul.f, ulnar facet; rad.f, radial facet. Foramina are labeled arbitrarily with lower-case letters (a to h). Unmarked punctures on dorsal and ventral surfaces may be bite marks. Scale bar, 2 cm.

pletely to different sides of the bone, thus minimizing the shoulder rotation that they can produce. In addition, the formation of an anteroposteriorly elongate strap-like humeral head implies that rotation at the shoulder was greatly restricted in *Panderichthys* and basal tetrapods. Therefore, the humerus of *Panderichthys* and basal tetrapods can be interpreted as being a broad platform for the insertion of extensor and flexor muscles that is less mobile than humeri of *Eusthenopteron* and other basal tetrapodomorphs.

The synapomorphies of more crownward tetrapod humeri, including ANSP 21350, correlate to a new orientation of the appendage on the body and an elaboration of the control of the distal limb skeleton. In all known early humeri, a ridge that runs perpendicular to the long axis of the humeral shaft is associated with a more laterally directed glenoid of the shoulder girdle. This suggests that the insertion of pectoralis musculature ran parallel to the body axis. The net effect of this new musculoskeletal arrangement is to minimize further the degree of shoulder level rotation during limb flexion. In addition, the expanded entepicondyle, elaborated surfaces around the epipodial facets, and extended ectepicondyle suggest enhanced distal limb musculature and motion.

With *Ichthyostega*, *Tulerpeton*, and *Acanthostega*, ANSP 21350 also reveals a diversity of limb design in the earliest tetrapods. The humeri of all known Devonian tetrapods differ in the size and orientation of entepicondyle, ectepicondyle, ventral ridge, and other areas for muscular insertion and origination. In particular, the limb of *Acanthostega* (*3*, *6*) contrasts with the others in that it is distinctly broad and flattened. In this appendage, the humerus is relatively gracile, the epipodial facets face distally, and, as in *Tulerpeton*, the ventral ridge is barely present. In this respect, ANSP 21350 represents a quite different functional design. Most of the processes, particularly those on the ventral surface (Fig. 2), are more robust and elaborate than those of *Acanthostega*. In addition, the ventral orientation of the epipodial facets contrasts with the more distal orientation of *Acanthostega*, *Panderichthys*, and *Eusthenopteron*. This ventral orientation implies that the limb of ANSP 21350 was limited in hyperextension and more flexed at the elbow than other Devonian taxa. The large epipodial facets, distally truncated yet massive entepicondyle, and elaborate distal areas for muscle attachment on ANSP 21350 indicate a greater range of ventrally directed motion for the radius and ulna than in *Acanthostega*. *Acanthostega* and ANSP 21350 represent two extremes of humeral design in the earliest tetrapods: one paddle-like, with a gracile humerus and distally facing epipodial facets, and the other with

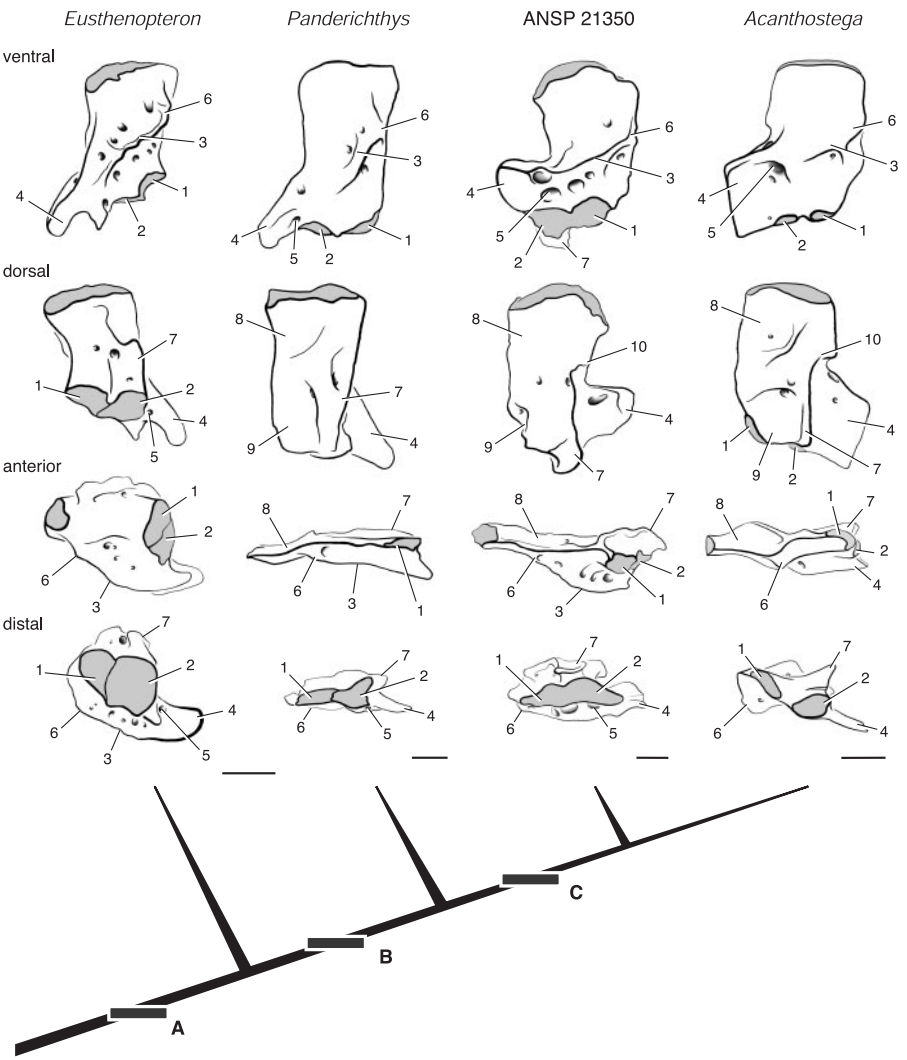

Fig. 2. Cladogram of stem group tetrapod humeri spanning the fin-to-limb transition, each in four standardized views (horizontal rows); relationship scheme after (*17*). The evolution of the tetrapod limb involved the compartmentalization of muscles, first dorsoventrally in outgroup fish and later proximodistally in early tetrapods. The first shift led to the separation of flexor and extensor muscles in tetrapods and their closest fish outgroups. Associated with this shift is the evolution of new surfaces for the attachment of muscles, a new flattened shape for the humeral body, and a new orientation between the major flexor and extensor muscles and the long axis of the humerus. At node A, primitive characters include a proximodistally short subcylindrical shaft with distally directed radial (1) and ulnal (2) articular surfaces; an oblique ventral ridge or crest (3) pierced by multiple foramina, extending posteriorly to a large entepicondylar process (4) with foramen (5, equivalent to a3 in Fig. 1), and anteriorly to a pectoral process (6); and dorsally, a rounded ectepicondylar ridge (7) is aligned with the ulnal facet. At node B, synapomorphies include a dorsoventrally flattened shaft; an enlarged and posteriorly inclined ectepicondylar ridge (7), a broad shallow depression proximally for scapulohumeral muscle insertion (8), and an enlarged area for muscle insertion above the radial condyle (9). At node C, synapomorphies include a distally extended ectepicondylar process (7); a distinct recess and incipient crest (10) at the proximal union of ectepicondylar and entepicondylar processes; an enlarged and proximodistally expanded entepicondylar process; and a ventral crest (3) confluent with the posteromedial rim of the entepicondylar process (4), thus subparallel to the long axis of the humeral head and dividing the ventral surface into proximal and distal compartments. The putative humerus of *Elginerpeton* (*18*) becomes difficult to interpret in light of these observations, because it has none of the synapomorphies shown in Fig. 2. By lacking the shared characters present in the most basal node, the identification of *Elginerpeton* as a tetrapod humerus would require both the evolution of unique features and the loss of all the apomorphies shared by tetrapods and their successive two outgroups. *Eusthenopteron foordi*, after (*5*); *Panderichthys rhombolepis*, after (*10*); *Acanthostega gunnari*, after (*3*).

robust flexor muscles at the shoulder and elbow, more permanent flexion at the elbow, and a greater range of motion distally.

Comparisons between the humeri of primitive fish and basal tetrapods reveal major functional stages in the origin of tetrapod limbs. The first important transformation happened in the common ancestor of panderichthyids and tetrapods: The humerus became a relatively immobile platform to support the body. The significance of this change is seen in correlated changes across the shoulder and humerus: in the expanded coracoid plate in the shoulder, the new flattened architecture of the humerus, the enhanced and reoriented muscular attachments, and the restricted rotatory movements possible at the articular surfaces of the shoulder. The new function of the appendage is not necessarily associated with adaptation to walking on land: Many of the changes seen in these Devonian taxa are also seen in modern fish, in which pectoral girdle enlargement, basal radial extension, and appendicular muscle elaboration are linked to trunk lifting and station holding in water (*14*, *15*). We argue that this function represents the intermediate condition between primitive steering and braking functions in fins (*4*, *16*) and the derived aquatic or terrestrial walking gait. In this regard, the origin of tetrapods involved the evolution of increased mobility in distal parts of paired appendages but the retention of restricted mobility proximally. Recent discoveries reveal an increasing functional diversity within these earliest stages of tetrapod evolution, implying that there likely will be a corresponding variety of trackway patterns attributable to tetrapods within Devonian rocks.

References and Notes

1. W. K. Gregory, H. C. Raven, *Ann. N. Y. Acad. Sci.* **42**, 273 (1941).
2. A. Romer, *Evolution* **12**, 365 (1958).
3. M. I. Coates. *Trans. R. Soc. Edinb.* **87**, 363 (1996).
4. J. A. Clack, *Gaining Ground: The Origin and Evolution of Tetrapods* (Indiana Univ. Press, Bloomington, IN, 2002).
5. S. M. Andrews, T. S. Westoll, *Trans. R. Soc. Edinb.* **68**, 207 (1970).
6. M. I. Coates, J. A. Clack, *Nature* **347**, 66 (1990).
7. E. Jarvik, *Fossils Strata* **40**, 1 (1996).
8. O. A. Lebedev, M. I. Coates, *Zool. J. Linn. Soc.* **114**, 307 (1995).
9. E. Vorobyeva, A. Kuznetsov, in *Fossil Fishes As Living Animals*, E. Mark-Kurik, Ed. (Academy of Sciences of Estonia, Tallin, Estonia, 1992).
10. E. Vorobyeva, *Paleontol. J.* **34**, 632 (2000).
11. A. Traverse, *Cour. Forschungsinst. Senckenb.* **241**, 19 (2003).
12. E. B. Daeschler, N. H. Shubin, K. S. Thomson, *Science* **265**, 639 (1994).
13. E. B. Daeschler, *J. Paleontol.* **74**, 301 (2000).
14. T. Goto, K. Nishida, K. Nakaya, *Ichthyol. Res.* **46**, 281 (1999).
15. C. D. Wilga, G. Lauder, *J. Morphol.* **249**, 195 (2001).
16. R. L. Carroll, *Vertebrate Paleontology and Evolution* (Freeman, New York, 1988).
17. P. E. Ahlberg, Z. Johanson, *Nature* **395**, 792 (1998).
18. P. E. Ahlberg, *Nature* **354**, 298 (1991).

19. R. Wadsworth enabled this research, K. Monoyios drew Fig. 2, and C. F. Mullison prepared the specimen. Supported by grants from NSF (grants EAR 0207721 and EAR 0208377 to N.H.S. and E.B.D.) and the National Geographic Society (to E.B.D. and N.H.S.).

3 December 2003; accepted 4 February 2004

Direct Activation of the ATM Protein Kinase by the Mre11/Rad50/Nbs1 Complex

Ji-Hoon Lee and Tanya T. Paull*

The complex containing the Mre11, Rad50, and Nbs1 proteins (MRN) is essential for the cellular response to DNA double-strand breaks, integrating DNA repair with the activation of checkpoint signaling through the protein kinase ATM (ataxia telangiectasia mutated). We demonstrate that MRN stimulates the kinase activity of ATM in vitro toward its substrates p53, Chk2, and histone H2AX. MRN makes multiple contacts with ATM and appears to stimulate ATM activity by facilitating the stable binding of substrates. Phosphorylation of Nbs1 is critical for MRN stimulation of ATM activity toward Chk2, but not p53. Kinase-deficient ATM inhibits wild-type ATM phosphorylation of Chk2, consistent with the dominant-negative effect of kinase-deficient ATM in vivo.

Eukaryotic cells respond to DNA damage with a rapid activation of signaling cascades that initiate from the ATR and ATM protein kinases. The response to DNA double-strand breaks (DSBs) occurs primarily through ATM and leads to phosphorylation of many targets critical for checkpoint activation, apoptosis, and DNA repair (*1*). One of the targets of ATM phosphorylation is the Nbs1 (nibrin) protein, which associates with the conserved DSB repair factors Mre11 and Rad50 (*2*). ATM phosphorylates Nbs1 on Ser-343 and other residues, modifications necessary for S-phase checkpoint activation and for survival of ionizing-radiation exposure (*3*–*8*).

The Nbs1 protein is not just a substrate of ATM, but also affects activation of ATM in response to DNA damage. The gene encoding Nbs1 is mutated in patients with the radiation sensitivity disorder Nijmegen breakage syndrome (NBS), characterized by chromosomal instability, radio-resistant DNA synthesis, and clinical phenotypes that include immunodeficiency and cancer (*9*). Cells from NBS patients do not produce full-length Nbs1 protein, and phosphorylation of Chk2, SMC1, and FANCD2 by ATM is reduced or absent in these cells (*7*, *8*, *10*–*14*). Thus, the MRN complex may participate in activating ATM to phosphorylate multiple other downstream substrates.

Department of Molecular Genetics and Microbiology, Institute of Cellular and Molecular Biology, University of Texas at Austin, 1 University Station, A4800, Austin, TX 78712, USA.

*To whom correspondence should be addressed. E-mail: tpaull@icmb.utexas.edu

To test this hypothesis, we measured the effects of MRN on ATM phosphorylation of Chk2, a protein kinase that activates S phase and mitotic checkpoints. ATM phosphorylates Chk2 on Thr-68 in response to DNA damage, which activates Chk2 to phosphorylate substrates including p53 and Cdc25C (*15*). Using a phospho-specific antibody specific for Chk2 Thr-68, we found that the addition of MRN to ATM stimulated Chk2 phosphorylation up to 15-fold (Fig. 1A). The activating effect of MRN was dependent on the absolute concentration of ATM in the reaction (Fig. 1B). Addition of Mre11/Rad50 (MR), lacking the Nbs1 protein, stimulated ATM phosphorylation of Chk2 only partially (Fig. 1C), indicating that Nbs1 is important for Chk2 activation.

Nbs1 phosphorylation on Ser-343 is required for ATM phosphorylation of substrates including Chk2, SMC1, and FANCD2 in vivo (*10*, *12*, *13*). To test the importance of Nbs1 phosphorylation for ATM stimulation, we used an S343A mutant version of Nbs1. The MRN(S343A) complex forms similarly to the wild-type (wt) complex and exhibits DNA binding and nuclease activities identical to those of the wt enzyme (*16*). The MRN(S343A) mutant complex did not stimulate ATM activity toward Chk2 in vitro (Fig. 1D). The presence of Nbs1 and phosphorylation of Ser-343 by ATM is therefore essential for MRN stimulation of ATM activity on Chk2. The complete absence of ATM stimulation by MRN(S343A) suggests that the presence of Nbs1 is inhibitory when Nbs1 cannot be phosphorylated.

Ataxia telangiectasia (A-T) patients lack functional ATM protein and exhibit